Eur. Phys. J. B (2015) 88: 273
DOI: 10.1140/epjb/e2015-60658-3

THE EUROPEAN PHYSICAL JOURNAL B

Regular Article

Electric field control of spin splitting in III-V semiconductor quantum dots without magnetic field

Sanjay Prabhakar[a] and Roderick Melnik

The MS2Discovery Interdisciplinary Research Institute, M^{2}NeT Laboratory, Wilfrid Laurier University, Waterloo, ON, N2L 3C5, Canada

Received 4 May 2015 / Received in final form 10 August 2015
Published online 26 October 2015 –

Abstract. We provide an alternative means of electric field control for spin manipulation in the absence of magnetic fields by transporting quantum dots adiabatically in the plane of two-dimensional electron gas. We show that the spin splitting energy of moving quantum dots is possible due to the presence of quasi-Hamiltonian that might be implemented to make the next generation spintronic devices of post CMOS technology. Such spin splitting energy is highly dependent on the material properties of semiconductor. It turns out that this energy is in the range of meV and can be further enhanced with increasing pulse frequency. In particular, we show that quantum oscillations in phonon mediated spin-flip behaviors can be observed. We also confirm that no oscillations in spin-flip behaviors can be observed for the pure Rashba or pure Dresselhaus cases.

1 Introduction

Several novel ways of spin manipulation in spintronic devices have been considered by different authors [1–9], having in mind their applications in the next generation optoelectronic devices that might be implemented for the realization of solid state quantum computing and quantum information processing [4,7,10,11]. Longer coherent times caused by phonon or electromagnetic radiation field in physical systems, such as quantum dots, quantum wells and quantum wires, are sought for getting high fedility quantum gates for the implementation in quantum information processing [2,12–14]. However, physical systems interact with the environmental noise and thus one can expect an exponential decay of the coherent time that might lose the behaviors of quantum phenomena, and hence might not be considered for applications in quantum information processing. Thus, several different techniques for different physical devices (quantum dots, cavity quantum electrodynamics and others) have been proposed to enhance the decoherence time [11–13,15]. Quantum circuits made from quantum dots in particular have potential interest because quantum dots with two ferromagnetic contacts can be efficiently used to inject electron spin in quantum dots with tuning gate controlled electric field along z-direction [7,10,11]. Contact-induced effective electric fields might be able to inject electron spin and to add switchable strong coupling to the cavity photons by using a standard technique known as cavity quantum electrodynamics [15]. Electric and magnetic field control of effective g-factor in isotropic and anisotropic semiconductor quantum dots is still considered to be the best choice by many researchers around the world because it is easy to grow and manipulate the spin in quantum dots with existing semiconductor state-of-the-art technology [7,9]. In these devices, one can tune the g-factor of electron and hole states with spin-orbit coupling coefficients in presence of externally applied magnetic and electric fields. Spin-orbit coupling in semiconductor consists of the Rashba and linear Dresselhaus couplings due to lack of structural inversion symmetry along the growth direction and bulk inversion symmetry in the crystal lattice. In this case we neglect the cubic Dresselhaus spin-orbit coupling due to its negligible contribution to the band structure of the unperturbed Hamiltonian in quantum dots [16,17]. However, for the case of quantum dots epitaxially grown in growth direction with no magnetic fields, spin-orbit coupling can modify some level of energy states but might become impossible to split the bands unless one can apply some level of trick to rotate the Hamiltonian operators in such a way that either Pauli x or y components of spin matrix couples to the z-component [18,19]. Then one might immediately argue that the spin-orbit couplings of the rotated Hamiltonian operator of quantum dots are not significantly strong to break the in-plane rotational symmetry and it might be impossible to induce Zeeman type spin splitting energy. Thus in this paper, we propose a more robust novel method to find the splitting

[a] e-mail: sprabhakar@wlu.ca

of the orbital states in quantum dots in the absence of magnetic fields. Here we apply the time dependent control field through gate potential in gated semiconductor quantum dots that allows us to investigate the spin manipulation in such structures. We assume that the quantum dots are transported adiabatically with the application of time dependent gate controlled electric fields and show that such moving quantum dots induce a quasi-Hamiltonian that breaks the in-plane rotational symmetry and induces spin-splitting energy even in the absence of magnetic fields. Then, we apply the Fermi Golden rule and estimate the spin relaxation time caused by piezo-phonons in moving quantum dots for applications in solid state quantum computing and quantum information processing. Although spin manipulation through geometric phases and realization of quantum gates by transporting III-V semiconductor quantum dots adiabatically have been studied in previous works [20,21], our goal here is to diagonalize the quantum dots Hamiltonian by degenerate and non-degenerate perturbation scheme and analyze the importance of the quasi-Hamiltonian on the bandstructures of quantum dots. Further realization of two-qubit quantum gates for holonomic quantum computers in solid state systems with and without magnetic fields has been studied in reference [21]. However, our work is different in that we may find resonant behaviors with the estimated decoherence rate ($\Gamma \approx (2T_1)^{-1} \sim \mu s^{-1}$) (see also Ref. [20]).

2 Theoretical model

For a moving semiconductor quantum dot (QD) in the plane of two-dimensional electron gas, we consider the total Hamiltonian $H = H_0 + H_{so}$ [21–23]. Here

$$H_0 = \frac{p_x^2 + p_y^2}{2m} + \frac{1}{2} m\omega_o^2 \left\{ (x - x_0)^2 + (y - y_0)^2 \right\}, \quad (1)$$

$$H_{so} = H_R + H_D = \frac{\alpha}{\hbar} (\sigma_x p_y - \sigma_y p_x) + \frac{\beta}{\hbar} (-\sigma_x p_x + \sigma_y p_y). \quad (2)$$

In equation (1), $\mathbf{p} = -i\hbar(\partial_x, \partial_y, 0)$ is the canonical momentum, m is the effective mass of an electron, $\omega_0 = \hbar/m\ell_0^2$ is the confining potential with ℓ_0 being the QDs radii, $x_0 = r_0 \cos\theta$, $y_0 = r_0 \sin\theta$ and $\theta = \omega t$. Here r_0 is the orbit radius and ω is the frequency of the control pulse. By varying θ very slowly, QD is adiabatically transported along the circular trajectory in the 2D plane. Equation (2) is the spin-orbit Hamiltonian consisting of the Rashba and the linear Dresselhaus couplings. In equation (2) $\alpha = \alpha_R eE$ and $\beta = 0.78\gamma_c \left(2me/\hbar^2\right)^{2/3} E^{2/3}$. Now we assume relative coordinate $\mathbf{R} = \mathbf{r} - \mathbf{r_0} = (X, Y, 0)$ and the relative momentum $\mathbf{P} = \mathbf{p} - \mathbf{p_0} = (P_X, P_Y, 0)$, where $\mathbf{p_0}$ is the momentum of the slowly moving quantum dot that might be classically given by $m\dot{\mathbf{r}}_0$. Thus we write the total Hamiltonian H in the form:

$$H(\mathbf{P}, \mathbf{R}) = H_0(\mathbf{P}, \mathbf{R}) + H_0'(x_0, y_0) + H_0''(\mathbf{P}, \mathbf{R}; x_0, y_0) + H_{so}(\mathbf{P}, \mathbf{R}) + H_q, \quad (3)$$

$$H_0(\mathbf{P}, \mathbf{R}) = \frac{P_X^2 + P_Y^2}{2m} + \frac{1}{2} m\omega_o^2 \left(X^2 + Y^2\right), \quad (4)$$

$$H_0'(x_0, y_0) = \frac{1}{2} m\omega^2 \left(x_0^2 + y_0^2\right) \quad (5)$$

$$H_0''(\mathbf{P}, \mathbf{R}; x_0, y_0) = -\omega (y_0 P_X - x_0 P_Y), \quad (6)$$

$$H_{so}(\mathbf{P}, \mathbf{R}) = \frac{\alpha}{\hbar} (\sigma_x P_Y - \sigma_y P_X) + \frac{\beta}{\hbar} (-\sigma_x P_X + \sigma_y P_Y), \quad (7)$$

$$H_q(x_0, y_0) = \frac{\alpha m\omega}{\hbar} (\sigma_x x_0 + \sigma_y y_0) + \frac{\beta m\omega}{\hbar} (\sigma_x y_0 + \sigma_y x_0). \quad (8)$$

We may also express $H_{so}(\mathbf{P}, \mathbf{R})$ and H_q in terms of the raising and lowering spin operators,

$$H_{so}(\mathbf{P}, \mathbf{R}) = \alpha \sqrt{\frac{m\omega_0}{\hbar}} (\sigma_+ a_+ - \sigma_- a_-) + \beta i \sqrt{\frac{m\omega_0}{\hbar}} (\sigma_- a_+ + \sigma_+ a_-) + H.c.. \quad (9)$$

$$H_q = \frac{m\omega}{\hbar} \left[\alpha (x_0 - i y_0) + \beta (y_0 - i x_0)\right] \sigma_+ + H.c, \quad (10)$$

where $\sigma_\pm = (\sigma_x \pm i\sigma_y)/2$ and $H.c.$ corresponds to Hermitian conjugate. We diagonalize Hamiltonian $H_0(\mathbf{P}, \mathbf{R})$ on the basis of the number states $|n_+, n_-\rangle$ as:

$$H_0 = (N_+ + N_- + 1)\hbar\omega_0, \quad (11)$$

where $N_\pm = a_\pm^\dagger a_\pm$ are the number operators with eigenvalues $n_\pm \in N_0$. Here,

$$a_\pm = \frac{1}{\sqrt{4m\hbar\omega_0}} (iP_X \pm P_Y) + \sqrt{\frac{m\omega_0}{4\hbar}} (X \mp iY), \quad (12)$$

$$a_\pm^\dagger = \frac{1}{\sqrt{4m\hbar\omega_0}} (-iP_X \pm P_Y) + \sqrt{\frac{m\omega_0}{4\hbar}} (X \pm iY), \quad (13)$$

provided that $\left[a_\pm, a_\pm^\dagger\right] = 1$. Now we consider H_0', H_0'', H_{so} and H_q as perturbation terms of H_0 and thus we write the eigenenergy of H as:

$$\varepsilon_{n_+n_-} = \varepsilon_{n_+n_-}^{(0)} + \varepsilon_{n_+n_-}^{(1)} + \tilde{\varepsilon}_{n_+n_-}^{(1)} + \varepsilon_{n_+n_-}^{(2)} + \tilde{\varepsilon}_{n_+n_-}^{(2)}, \quad (14)$$

where the unperturbed energy eigenvalues of H_0 are

$$\varepsilon_{n_+n_-}^{(0)} = (n_+ + n_- + 1)\hbar\omega_0, \quad (15)$$

and the first order energy corrections are

$$\varepsilon_{n_+n_-}^{(1)} = \langle n_+n_-|H_0'|n_+n_-\rangle = m\omega^2 r_0^2/2 = G, \quad (16)$$

$$\tilde{\varepsilon}_{n_+n_-}^{(1)} = \langle n_+n_-|H_q|n_+n_-\rangle = \frac{m\omega}{\hbar} \left[\alpha (x_0 - i y_0) + \beta (y_0 - i x_0)\right] \sigma_+ + H.c., \quad (17)$$

$$\begin{vmatrix} \varepsilon^{(0)}_{n_+n_-} + \varepsilon^{(1)}_{n_+n_-} + \varepsilon^{(2)}_{n_+n_-} + \tilde{\varepsilon}^{(2)+}_{n_+n_-} - \varepsilon_{n_+n_-} & \frac{\alpha m\omega}{\hbar}(x_0 - iy_0) + \frac{\beta m\omega}{\hbar}(y_0 - ix_0) \\ \frac{\alpha m\omega}{\hbar}(x_0 + iy_0) + \frac{\beta m\omega}{\hbar}(y_0 + ix_0) & \varepsilon^{(0)}_{n_+n_-} + \varepsilon^{(1)}_{n_+n_-} + \varepsilon^{(2)}_{n_+n_-} + \tilde{\varepsilon}^{(2)-}_{n_+n_-} - \varepsilon_{n_+n_-} \end{vmatrix} = 0 \quad (22)$$

and the second order energy corrections are

$$\varepsilon^{(2)}_{n_+n_-} = \sum_{m_+m_- \neq n_+n_-} \frac{|\langle m_+m_-|H_0''|n_+n_-\rangle|^2}{\varepsilon^0_{n_+n_-} - \varepsilon^0_{m_+m_-}}, \quad (18)$$

$$\tilde{\varepsilon}^{(2)}_{n_+n_-} = \sum_{m_+m_- \neq n_+n_-} \frac{|\langle m_+m_-|H_{so}|n_+n_-\rangle|^2}{\varepsilon^0_{n_+n_-} - \varepsilon^0_{m_+m_-}}, \quad (19)$$

where

$$\begin{aligned} \langle m_+m_-|H_0''|n_+n_-\rangle &= \omega\sqrt{\frac{m\hbar\omega_0}{4}} \\ &\times \Big\{ (iy_0 + x_0)\sqrt{n_+}\delta_{m_+m_-,(n_+-1)n_-} \\ &+ (-iy_0 + x_0)\sqrt{n_+ + 1}\delta_{m_+m_-,(n_++1)n_-} \\ &+ (iy_0 - x_0)\sqrt{n_-}\delta_{m_+m_-,n_+(n_--1)} \\ &+ (-iy_0 - x_0)\sqrt{n_- + 1}\,\delta_{m_+m_-,n_+(n_-+1)}\Big\}, \end{aligned} \quad (20)$$

$$\begin{aligned} \langle m_+m_-|H_{so}|n_+n_-\rangle &= \sqrt{\frac{m\omega_0}{\hbar}} \\ &\times \Big\{ (\alpha\sigma_+ + i\beta\sigma_-)\sqrt{n_+}\delta_{m_+m_-,(n_+-1)n_-} \\ &+ (\alpha\sigma_- - i\beta\sigma_+)\sqrt{n_+ + 1}\delta_{m_+m_-,(n_++1)n_-} \\ &- (\alpha\sigma_- - i\beta\sigma_+)\sqrt{n_-}\delta_{m_+m_-,n_+(n_--1)} \\ &- (\alpha\sigma_+ + i\beta\sigma_-)\sqrt{n_- + 1}\,\delta_{m_+m_-,n_+(n_-+1)}\Big\}. \end{aligned} \quad (21)$$

Note that the matrix element (21) multiplied with its Hermitian conjugate provides us the terms containing either $\sigma_+\sigma_-$ or $\sigma_-\sigma_+$ which are the elements of the diagonal matrix (see Appendix A. Finally, we express (14) as

see equation (22) above,

where $\tilde{\varepsilon}^{(2)\pm}_{n_+n_-}$ correspond to the energy correction terms of the upper and lower elements of the diagonal matrix (for details, see Appendix A). Now it is straight forward to find the energy eigenvalues of (22) as:

$$\begin{aligned} 2\varepsilon_{n_+n_-\pm} &= E_{n_+n_-} \pm \Big[E^2_{n_+n_-} - 4\Big\{\tilde{\tilde{\varepsilon}}^2_{n_+n_-} \\ &+ \tilde{\tilde{\varepsilon}}_{n_+n_-}\left(\tilde{\varepsilon}^{(2)+}_{n_+n_-} + \tilde{\varepsilon}^{(2)-}_{n_+n_-}\right) + \tilde{\varepsilon}^{(2)+}_{n_+n_-}\tilde{\varepsilon}^{(2)-}_{n_+n_-} - \omega^2\kappa^2\Big\}\Big]^{1/2}, \end{aligned} \quad (23)$$

where $s = \pm$ correspond to the eigenvalues associated to spin up and down states and

$$E_{n_+n_-} = 2\tilde{\tilde{\varepsilon}}_{n_+n_-} + \tilde{\varepsilon}^{(2)+}_{n_+n_-} + \tilde{\varepsilon}^{(2)-}_{n_+n_-}, \quad (24)$$

$$\tilde{\tilde{\varepsilon}}_{n_+n_-} = \varepsilon^{(0)}_{n_+n_-} + \varepsilon^{(1)}_{n_+n_-} + \varepsilon^{(2)}_{n_+n_-}, \quad (25)$$

$$\kappa = \frac{m}{\hbar}\left[(\alpha x_0 + \beta y_0)^2 + (\alpha y_0 + \beta x_0)^2\right]^{1/2}. \quad (26)$$

We noticed from (23) that the bandstructures of quantum dots explicitly depend on the adiabatic parameters, x_0 and y_0 that induce resonant behaviors on the energy eigenvalues of spin splitting during the adiabatic movement of the dots in the plane of 2-dimensional electron gas. Also, from (26) either for the pure Rashba case (i.e., $\beta = 0$), we find $k = m\alpha/\hbar$ or for the pure Dresselhaus case (i.e., $\alpha = 0$), we find $k = m\beta/\hbar$ which is completely independent from the periodic potential that we apply electrically to let the dots to move in a circular trajectory. Thus either for the pure Rashba or Dresselhaus cases (i.e., only one type of spin-orbit interaction present), we might not find any resonant behaviors. The distribution of the charge density is expected to be constant along the transported route (circular trajectory) of the dots either for the pure Rashba or pure Dresselhaus cases [24]. Hence the resonant peaks can only be observed for the cases of the interplay between the Rashba and Dresselhaus spin-orbit couplings that might provide an evidence of broken in-plane rotational symmetry in quantum dots. For $\hbar\omega_0 >> G$, we may express $\Delta \propto \kappa\omega$ (see Appendix A for details) and for a special case, $\alpha = \beta$, we may also write $\Delta \propto m\alpha r_0 \sin 2\theta/\hbar$ (see also Ref. [24]). Therefore, large spin-orbit coupling strengths lead to strong localization of electrons (anisotropic effect) along z-direction at the heterojunction and the spin splitting energy difference exhibits minima at the valleys of the $\sin 2\theta$ potential (i.e., at $\theta = 3\pi/4$ or $7\pi/4$) or maxima at $\theta = \pi/4$ or $5\pi/4$ (see Fig. 1). Similar kind of periodic potential term $\Delta \propto \sin\theta$ may also appear for the case of quantum dots whose axis of orientation is considered at the origin (i.e., $r_0 = 0$ in our theoretical model) where interplay between Rashba-Dresselhaus spin-orbit couplings break the rotational symmetry and persistent spin current may be observed (see Ref. [24] for details).

Now we estimate the spin relaxation time caused by the emission of one piezo-phonon at absolute zero temperature between two lowest energy states in III-V semiconductor QDs [25]. Hence, the coupling between an electron and a piezo-phonon with mode $\mathbf{q}\alpha$ ($\mathbf{q}$ is the phonon wave vector and the branch index $\alpha = l, t_1, t_2$

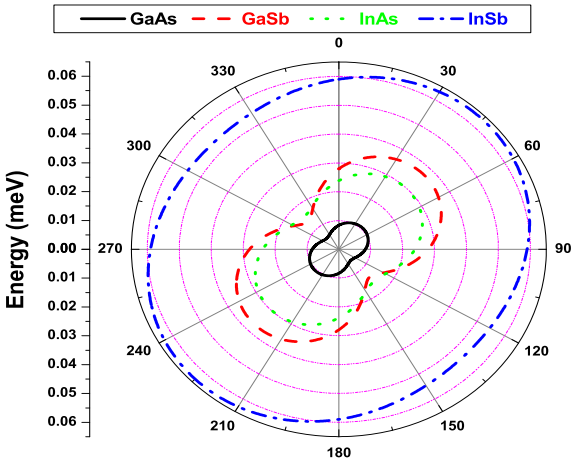

Fig. 1. Spin splitting energy difference vs. rotation angle in III-V semiconductor quantum dots. Here we chose $r_0 = 50$ nm, $\omega = 100$ GHz, $\ell_0 = 32$ nm and $E = 10^5$ V/cm. Other material constants are chosen from reference [4].

for one longitudinal and two transverse modes) is given by [4,25,26]:

$$u_{\rm ph}^{\mathbf{q}\alpha}(\mathbf{r},t) = \sqrt{\frac{\hbar}{2\rho V\omega_{\mathbf{q}\alpha}}}e^{i(\mathbf{q}\cdot\mathbf{r}-\omega_{q\alpha}t)}eA_{\mathbf{q}\alpha}b_{\mathbf{q}\alpha}^{\dagger} + H.c., \quad (27)$$

where ρ is the crystal mass density, V is the volume of the QD and $A_{\mathbf{q}\alpha} = \hat{q}_i\hat{q}_k e\beta_{ijk}e_{\mathbf{q}\alpha}^{j}$ is the amplitude of the electric field created by phonon strain. Here $\hat{\mathbf{q}} = \mathbf{q}/q$ and $e\beta_{ijk} = eh_{14}$ for $i \neq k, i \neq j, j \neq k$. Based on the Fermi Golden Rule, the phonon induced spin transition rate in the QDs is given by [25,26]

$$\frac{1}{T_1} = \frac{2\pi}{\hbar}\int\frac{d^3\mathbf{q}}{(2\pi)^3}\sum_{\alpha=l,t}|M(\mathbf{q}\alpha)|^2\delta(\hbar s_\alpha\mathbf{q} - \Delta), \quad (28)$$

where $\Delta = \varepsilon_{00+} - \varepsilon_{00+}$ (see Appendix A) and the matrix element $M(\mathbf{q}\alpha) = \langle\psi_i|u_{ph}^{\mathbf{q}\alpha}(\mathbf{r},t)|\psi_f\rangle$ has been calculated perturbatively [4,9,27]. Here $|\psi_i\rangle$ and $|\psi_f\rangle$ correspond to the initial and finial states of the Hamiltonian H. Based on second order perturbation theory, the spin relaxation time caused by phonon is given by:

$$\frac{1}{T_1} = \frac{4(eh_{14})^2\Delta^3}{35\pi\hbar^5\rho}\left(\frac{1}{s_l^5} + \frac{4}{3}\frac{1}{s_t^5}\right)\frac{G^2(\alpha^2+\beta^2)}{\left[(\hbar\omega_0)^2 - G^2\right]^2}. \quad (29)$$

Clearly, relaxation rate depends on Δ which is proportional to the periodic potential term $\sin\theta$ and $\cos\theta$ (also see Appendix A). Thus, we expect quantum oscillations (see Fig. 3) in the relaxation rate during the adiabatic transport of the quantum dots.

3 Results and discussions

By analyzing equation (23) (see also Eq. (A.13)), we find that the quasi-Hamiltonian induces spin splitting energy in a moving QD which is similar to the Landau levels in the presence of magnetic fields. In Figure 1, we plot the spin splitting energy difference vs. rotation angle of III-V semiconductor quantum dots. Such spin splitting energy is highly dependent on the Rashba-Dresselhaus spin-orbit coupling coefficients and on the control frequency ω. In Figure 2, at any fixed time interval, the quantum dots, displaced from its center, also allows us to investigate the interplay between the Rashba-Dresslhaus spin-orbit couplings on the energy spectrum of the dots. We clearly see that for the case of InSb QDs, large spin orbit couplings induce large gaps over other materials (GaAs, GaSb, InAs). Since spin-orbit couplings themselves induce an anisotropy effect (see Refs. [24,27]), the enhancement in the spin splitting energy difference by tuning both the Rashba-Dresselhaus spin-orbit couplings may provide an evidence of broken in-plane rotational symmetry. For the case of 100 GHz, the spin splitting energy is comparable to the Landau energy levels at large spin-orbit coupling coefficients (see Fig. 2) and might be utilized to break the in-plane rotational symmetry. The splitting of s- and p-states of quantum dots due to the presence of quasi-Hamiltonian allows us to investigate several physical phenomena by estimating the decoherence time (current motivation of our work), as well as to robustness of spin manipulation through Berry phase for topological quantum computing and other spintronics [20–23,28]. In Figure 3, we plot the spin relaxation rate caused by piezo-phonon vs. time in a moving quantum dot. It can be seen that the behavior of spin relaxation is a sinusoidal function due to the fact that the spin relaxation explicitly depends on $\sin(2\theta)$ (see Eq. (29)). Here we find that at $t = 0$, the spin relaxation does not vanish because at $\theta = 0$, the QD displaced from center $r_0 = 0$ to r_0 and thus the quasi-Hamiltonian (i.e. the off diagonal terms of Eq. (22)) induces appreciable values of spin splitting energy. In Figure 4, we plot phonon mediated spin relaxation vs. QDs radii. Here we find that the cusp-like structure can be observed with the accessible values of the QDs radii due to the accidental degeneracy point in equation (29). Cusp-like structure can be found exactly with the expression: $\ell_0 = 1.42\hbar/(m\omega r_0)$. At or near the cusp-like structure, the spin-relaxation rate is greatly enhanced that reduces the decoherence time. As a result, accidental degeneracy point may not be considered as an ideal location for the design of spintronic devices for quantum information processing. This avoided ideal location is similar to the spin hot spot that was described in references [2,4,27,29] but differs in that even in the absence of the magnetic field, quasi-Hamiltonian due to time dependent electric field control parameter also induces the accidental degeneracy point in the energy spectrum of electron in a moving QD.

4 Conclusion

We have proposed a theoretical model for the spin splitting of electron in semiconductor quantum dots without applying any source of magnetic fields. In Figures 1 and 2,

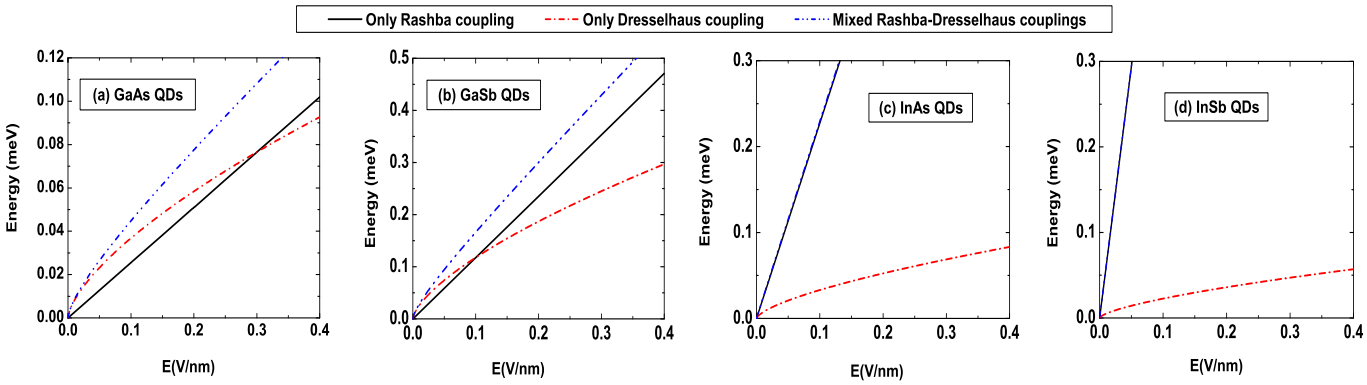

Fig. 2. Spin splitting energy difference vs. electric field in III-V semiconductor quantum dots. Note that applied electric field determine the strength of the Rashba and Dresselhaus spin-orbit couplings. Interplay between the Rashba and Dresselhaus spin-orbit couplings induce large gaps in the energy spectrum of quantum dots that may provide an evidence of broken in-plane rotational symmetry (see also Ref. [24]).

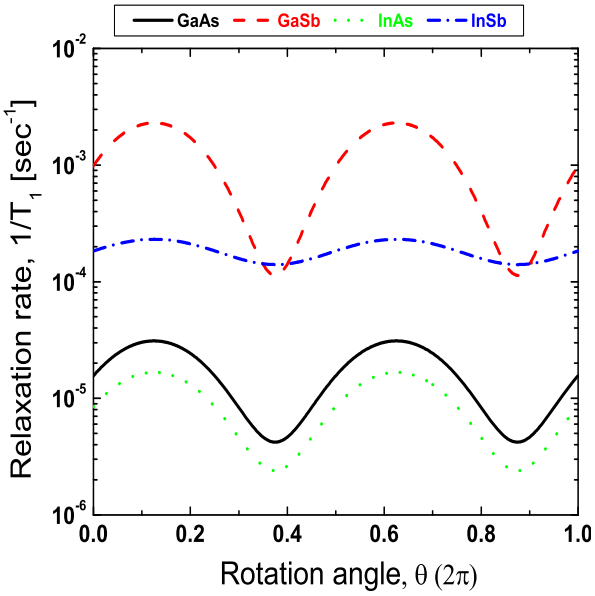

Fig. 3. Relaxation rate mediated by phonon vs. time in III-V semiconductor quantum dots. Here we chose $r_0 = 100$ nm, $\omega = 10$ GHz, $\ell_0 = 32$ nm and $E = 10^5$ V/cm. Other material constants are chosen from reference [4].

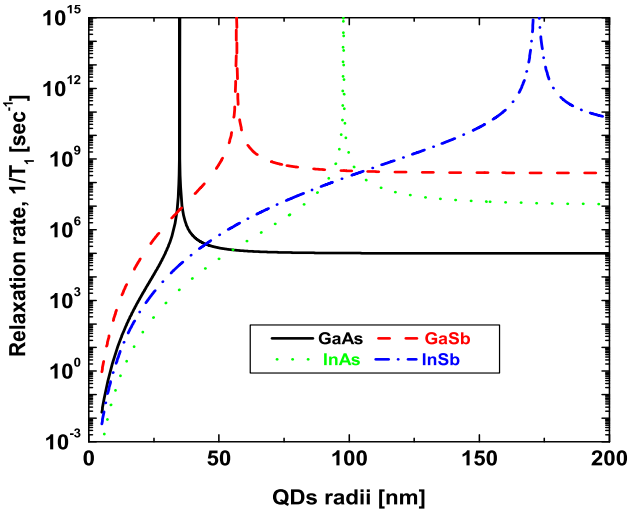

Fig. 4. Relaxation rate mediated by phonon vs. QDs radii in III-V semiconductor quantum dots. Here we chose $\theta = 0$, $r_0 = 100$ nm, $\omega = 700$ GHz, and $E = 10^4$ V/cm. Other material constants are chosen from reference [4].

This work was supported by NSERC and CRC programs, Canada.

we have shown that the spin splitting energy of III-V semiconductor quantum dots is possible even in the absence of magnetic fields. The spin splitting is observed due to the presence of quasi-Hamiltonian that does not depend on momentum and position operators but depends on the Pauli spin operator in a moving QD. In Figure 3, we have shown that the quantum oscillations and dips in the phonon mediated spin relaxation are observed in a fixed time interval. Finally, in Figure 4, we have shown that the cusp-like structure due to accidental degeneracy in the energy spectrum of quantum dots in the phonon mediated spin relaxation is seen and one might need to avoid such a location for the design of spintronic devices for quantum information processing.

Appendix A: Estimation of spin splitting of lowest energy eigenvalues

For the lowest state, we assume the quantum numbers $n_+n_- = 00$ and write the eigenvalues from (15) and (16) as:

$$\varepsilon_{00}^{(0)} = \hbar\omega_0, \tag{A.1}$$

$$\varepsilon_{00}^{(1)} = \frac{1}{2}m\omega^2 r_0^2 = G. \tag{A.2}$$

To find $\varepsilon_{00}^{(2)}$ and $\tilde{\varepsilon}_{00}^{(2)}$ from (18) and (19), we notice that unperturbed energy $\varepsilon_{m_+m_-}^{(0)}$ $(m_+m_- \neq n_+n_-)$ for 01 or 10

are degenerate. Thus, we apply degenerate perturbation theory and write

$$\varepsilon_{01}^{(0)} = \varepsilon_{01}^{(0)-} = 2\hbar\omega_0 - G, \tag{A.3}$$

$$\varepsilon_{10}^{(0)} = \varepsilon_{10}^{(0)+} = 2\hbar\omega_0 + G. \tag{A.4}$$

Next we write $\varepsilon_{00}^{(2)}$ from (18) as:

$$\varepsilon_{00}^{(2)} = \frac{|\langle 01|H_0''|00\rangle|^2}{\varepsilon_{00}^0 - \varepsilon_{01}^{(0)-}} + \frac{|\langle 10|H_0''|00\rangle|^2}{\varepsilon_{00}^0 - \varepsilon_{10}^{(0)+}}, \tag{A.5}$$

$$= -\frac{G\left(\hbar\omega_0\right)^2}{\left(\hbar\omega_0\right)^2 - G^2}. \tag{A.6}$$

Also we write $\tilde{\varepsilon}_{00}^{(2)}$ from (19) as:

$$\tilde{\varepsilon}_{00}^{(2)} = \frac{|\langle 01|H_{so}''|00\rangle|^2}{\varepsilon_{00}^0 - \varepsilon_{01}^{(0)-}} + \frac{|\langle 10|H_{so}''|00\rangle|^2}{\varepsilon_{00}^0 - \varepsilon_{10}^{(0)+}}. \tag{A.7}$$

By considering

$$|\langle 01|H_{so}|00\rangle|^2 = \frac{m\omega_0}{\hbar}\left(\alpha^2\sigma_+\sigma_- + \beta^2\sigma_-\sigma_+\right)$$

$$= \frac{m\omega_0}{\hbar}\begin{pmatrix}\alpha^2 & 0\\ 0 & \beta^2\end{pmatrix}, \tag{A.8}$$

$$|\langle 10|H_{so}|00\rangle|^2 = \frac{m\omega_0}{\hbar}\left(\alpha^2\sigma_-\sigma_+ + \beta^2\sigma_+\sigma_-\right)$$

$$= \frac{m\omega_0}{\hbar}\begin{pmatrix}\beta^2 & 0\\ 0 & \alpha^2\end{pmatrix}, \tag{A.9}$$

we write $\tilde{\varepsilon}_{00}^{(2)}$ from (A.7) as:

$$\tilde{\varepsilon}_{00}^{(2)} = \begin{pmatrix}\tilde{\varepsilon}_{00}^{(2)+} & 0\\ 0 & \tilde{\varepsilon}_{00}^{(2)-}\end{pmatrix}, \tag{A.10}$$

where

$$\tilde{\varepsilon}_{00}^{(2)+} = -\frac{m\omega_0}{\hbar}\left[\frac{\alpha^2}{\hbar\omega_0 - G} + \frac{\beta^2}{\hbar\omega_0 + G}\right], \tag{A.11}$$

$$\tilde{\varepsilon}_{00}^{(2)-} = -\frac{m\omega_0}{\hbar}\left[\frac{\beta^2}{\hbar\omega_0 - G} + \frac{\alpha^2}{\hbar\omega_0 + G}\right]. \tag{A.12}$$

Considering $n_+n_- = 00$, we re-write (23) as:

$$\varepsilon_{00\sigma_z} = (1-\delta)\,\hbar\omega_0 + \omega\kappa\sigma_z, \tag{A.13}$$

where $\delta(<1) = (m\omega_0/\hbar)(\alpha_R^2 + \alpha_D^2)/[(\hbar\omega_0)^2 - G^2]$. In (A.13), we have neglected the term associated to $\tilde{\varepsilon}_{00}^{(2)+} \cdot \tilde{\varepsilon}_{00}^{(2)-} \ll 1$. The perturbation scheme to diagonalize total H works for the case when the perturbed energy eigenvalues are smaller than the unperturbed energy eigenvalues. For example, the parameters chosen in Figure 1 for GaAs case at $\theta = 0$, we estimate $\varepsilon_{00}^{(0)} \approx 1.1$ meV, $\varepsilon_{00}^{(1)} \approx -\varepsilon_{00}^{(2)} \approx 4.7$ μeV, $\tilde{\varepsilon}_{00}^{(2)+} \approx -1.81$ μeV and $\tilde{\varepsilon}_{00}^{(2)-} \approx -1.83$ μeV. Evidently, the perturbed energy eigenvalues depend on the control pulse frequency ω, and orbit radius r_0, where quantum dots move adiabatically along the circular trajectory. For larger values of ω and r_0, the perturbation scheme to diagonalize the total H may not work and the adiabaticity theorem may not be valid (see below).

The quantum dots must be transported very slowly so that we can apply the adiabatic theorem. The criteria of the adiabaticity puts a limit on the classical velocity $v = \dot{r}$ of the moving quantum dot in order to keep the electron in its ground state. By considering the spin-orbit length $\lambda_{R,D} = \hbar^2/m\alpha_{R,D}$, we need to satisfy $\Gamma\lambda_{so} \ll |v| \ll \ell_d\omega_0$ at any moment in time. Here R, D correspond to the Rashba and Dresselhaus cases, $\Gamma \approx (2T_1)^{-1}$ is the decoherence rate, $\ell_d = 2\ell_0$ is the size of the dot. By considering the parameters chosen in Figure 3 at $\theta = 0$ for GaAs, we find $\Gamma = 8$ μs^{-1}, $\lambda_R = 2.6$ μm, $\lambda_D = 0.83$ μm (the values approximately match to Refs. [20,21]) and estimate that $\Gamma\lambda_{so} = 0.014$ nm/s and $\ell_d\omega_0 = 10^{14}$ nm/s. Finally, we find $v = \sqrt{v_x^2 + v_y^2} = r_0\omega = 10^{12}$ nm/s at $\theta = 0$ which is in the range of adiabaticity condition mentioned above. In other words, $\omega \ll \omega_0$ to satisfy the adiabatic condition for the movement of the quantum dots. For experimental set up, we expect similar to references [7,30] but the QDs must be transported very slowly by obeying the criteria of the adiabaticity (also see Refs. [20,21,23,28]).

References

1. C.E. Pryor, M.E. Flatté, Phys. Rev. Lett. **96**, 026804 (2006)
2. D.V. Bulaev, D. Loss, Phys. Rev. Lett. **95**, 076805 (2005)
3. S. Das Sarma, M. Freedman, C. Nayak, Phys. Rev. Lett. **94**, 166802 (2005)
4. S. Prabhakar, R. Melnik, L.L. Bonilla, Phys. Rev. B **87**, 235202 (2013)
5. D.D. Awschalom, D. Loss, N. Samarth, *Semiconductor Spintronics and Quantum Computation* (Springer, Berlin, 2002)
6. D. Loss, D.P. DiVincenzo, Phys. Rev. A **57**, 120 (1998)
7. S. Takahashi, R.S. Deacon, K. Yoshida, A. Oiwa, K. Shibata, K. Hirakawa, Y. Tokura, S. Tarucha, Phys. Rev. Lett. **104**, 246801 (2010)
8. S. Prabhakar, J.E. Raynolds, Phys. Rev. B **79**, 195307 (2009)
9. S. Prabhakar, J.E. Raynolds, R. Melnik, Phys. Rev. B **84**, 155208 (2011)
10. S. Bandyopadhyay, Phys. Rev. B **61**, 13813 (2000)
11. S. Amasha, K. MacLean, I.P. Radu, D.M. Zumbühl, M.A. Kastner, M.P. Hanson, A.C. Gossard, Phys. Rev. Lett. **100**, 046803 (2008)
12. M. Kroutvar, Y. Ducommun, D. Heiss, M. Bichler, D. Schuh, G. Abstreiter, J.J. Finley, Nature **432**, 81 (2004)
13. J.M. Elzerman, R. Hanson, L.H. Willems van Beveren, B. Witkamp, L.M.K. Vandersypen, L.P. Kouwenhoven, Nature **430**, 431 (2004)

14. T.S. Koh, S.N. Coppersmith, M. Friesen, Proc. Natl. Acad. Sci. **110**, 19695 (2013)
15. A. Cottet, T. Kontos, Phys. Rev. Lett. **105**, 160502 (2010)
16. Y.A. Bychkov, E.I. Rashba, J. Phys. C **17**, 6039 (1984)
17. G. Dresselhaus, Phys. Rev. **100**, 580 (1955)
18. S. Prabhakar, R. Melnik, L.L. Bonilla, J. Phys. D **46**, 265302 (2013)
19. S.I. Erlingsson, J.C. Egues, D. Loss, Phys. Rev. B **82**, 155456 (2010)
20. P. San-Jose, B. Scharfenberger, G. Schön, A. Shnirman, G. Zarand, Phys. Rev. B **77**, 045305 (2008)
21. V.N. Golovach, M. Borhani, D. Loss, Phys. Rev. A **81**, 022315 (2010)
22. S. Prabhakar, R. Melnik, A. Inomata, Appl. Phys. Lett. **104**, 142411 (2014)
23. S. Prabhakar, R. Melnik, L.L. Bonilla, Phys. Rev. B **89**, 245310 (2014)
24. J.S. Sheng, K. Chang, Phys. Rev. B **74**, 235315 (2006)
25. A.V. Khaetskii, Y.V. Nazarov, Phys. Rev. B **64**, 125316 (2001)
26. R. de Sousa, S. Das Sarma, Phys. Rev. B **68**, 155330 (2003)
27. S. Prabhakar, R.V.N. Melnik, L.L. Bonilla, Appl. Phys. Lett. **100**, 023108 (2012)
28. Y. Ban, X. Chen, E.Y. Sherman, J.G. Muga, Phys. Rev. Lett. **109**, 206602 (2012)
29. D.V. Bulaev, D. Loss, Phys. Rev. B **71**, 205324 (2005)
30. M. Pechal, S. Berger, A.A. Abdumalikov, J.M. Fink, J.A. Mlynek, L. Steffen, A. Wallraff, S. Filipp, Phys. Rev. Lett. **108**, 170401 (2012)